



ELSEVIER

Earth and Planetary Science Letters 121 (1994) 1–18

EPSL

## Cooling of the Earth in the Archaean: Consequences of pressure-release melting in a hotter mantle

N.J. Vlaar, P.E. van Keken, A.P. van den Berg

*Department of Theoretical Geophysics, Institute of Earth Sciences, PO Box 80.021, 3508 TA Utrecht, The Netherlands*

(Received June 29, 1993; revision accepted October 12, 1993)

### Abstract

A model is presented to describe the cooling of the Earth in the Archaean. At the higher Archaean mantle temperatures pressure-release melting starts deeper and generates a thicker basaltic or komatiitic crust and depleted harzburgite layer compared with the present-day situation. Intrinsic compositional stability and lack of mechanical coherency renders the mechanism of plate tectonics ineffective. It is proposed that the Archaean continents stabilised early on top of a compositionally stratified root. In the Archaean oceanic lithosphere, hydrated upper crust can founder and recycle through its high-pressure phase eclogite. Eclogite remelting and new pressure-release melting generates new crustal material. Migration of magma and latent heat release by solidification at the surface provides an efficient mechanism to cool the mantle by several hundreds of degrees during the Archaean. This can satisfactorily explain the occurrence of high extrusion temperature komatiites and lower extrusion temperature basalts in greenstone belts as being derived from the same source by different mechanisms.

### 1. Introduction

There is still considerable controversy over the mantle temperature during the Archaean (ca. 3.5–2.7 Gyr B.P.). On the one hand, high mantle temperatures are inferred from the occurrence of very magnesian komatiitic lavas that are widespread in most Archaean greenstone belts, but rarely found after the Archaean–Proterozoic transition at 2.7 Gyr. These komatiites indicate high extrusion temperatures and melting temperatures some 400–500 K in excess of today's man-

tle temperatures. Some have taken this an indicating the average mantle temperatures [1–3]. Others assume the average mantle temperature to have been only 200–300 K higher than at present [4–6] and take the occurrence of komatiites to be the consequence of hotspot activity. A third group proposes even lower temperatures for the Archaean [7]. On the other hand, however, temperatures down to the 50 km depth in the Archaean continents, as have been derived from high-grade terrains, indicate conditions that have not been very different from the present-day situation. This 'Archaean paradox' has led many investigators to models in which cooling of the hotter Earth took place through rapid convection beneath the oceans. In most of these model stud-

[vdV]

ies it is implicitly assumed that mantle convection models can simulate present-day plate-tectonic processes, and that plate tectonics has been operative in the Archaean [4,8–10]. However, the present-day tectonic plate forces of slab pull and ridge push [64] are strongly dependent on lithospheric age and hence on lithospheric recycling rate and mantle temperature. A uniformitarian extrapolation of present conditions to the Archaean may not be valid [3,11] and therefore a different approach must be adopted.

We will first consider some previously published thermal cooling models of the Earth which have been used to constrain Archaean mantle temperatures. Next, the influence of higher temperatures on the pressure-release melting of mantle diapirs, and the related changes in upper mantle dynamics, are considered. Finally, we will present a model for the dynamics of the oceanic lithosphere and discuss its applicability to the cooling of the Earth in the Archaean.

## 2. Cooling models for the Earth based on parameterised convection

Several authors have studied thermal histories of the Earth using parameterised mantle convection models. This section discusses some of the approaches and approximations that have been used. Our discussion of this is not meant to be complete or to add new insights. In the studies mentioned the change of average mantle temperature with time follows from the energy balance equation:

$$\begin{aligned} \frac{4\pi}{3}\rho c_p(R_m^3 - R_c^3)\frac{dT}{dt} \\ = -4\pi qR_m^2 + \frac{4\pi}{3}Q(R_m^3 - R_c^3) \end{aligned} \quad (1)$$

where  $q$  is the average heat flux out of the Earth's surface and  $Q$  is the average heat production in the mantle. The definition of the other parameters is given in Table 1. The heat flux from the core into the base of the lower mantle has been assumed to be small [12] and is disregarded by most authors. For the mantle the Nus-

Table 1  
Notation and nominal values

Parameter	Definition	Value
$g$	gravitational acceleration	$9.8 \text{ ms}^{-2}$
$\alpha$	thermal expansivity	$3 \times 10^{-5} \text{ K}^{-1}$
$\kappa$	thermal diffusivity	$10^{-6} \text{ m}^2\text{s}^{-1}$
$D$	Depth of convection layer	$2.8 \times 10^6 \text{ m}$
$\nu$	kinematic viscosity	
$\eta$	dynamic viscosity	
$\nu_0$	Minimum kinematic viscosity	$2.21 \times 10^7 \text{ m}^2\text{s}^{-1}$
$A$	Activation temperature ( $\gamma T_m$ )	$5.6 \times 10^4 \text{ K}$
$k$	thermal conductivity	$4.2 \text{ Wm}^{-1}\text{K}^{-1}$
$\rho c_p$	volumetric specific heat	$4.2 \times 10^6 \text{ Jm}^{-3}\text{K}^{-1}$
$R_c$	core radius	$3.471 \times 10^6 \text{ m}$
$R_m$	mantle outer radius	$6.271 \times 10^6 \text{ m}$
$Ra_c$	critical Rayleigh number	1100
$T_S$	surface temperature	273 K
$\beta$	power law exponent	0.3

selt number  $Nu$  can be defined as the ratio of the total heat flux to the conductive heat flux out of the mantle:

$$Nu = (q_{\text{cond}} + q_{\text{conv}})/q_{\text{cond}} = qD/k\Delta T \quad (2)$$

where  $\Delta T$  is the temperature difference across the mantle. The relation between the Nusselt number and the vigour of convection in the mantle, which has been exploited in parameterised convection models, is

$$Nu = (Ra/Ra_c)^\beta \quad (3)$$

where  $Ra$  is the mantle Rayleigh number and  $Ra_c$  is the critical Rayleigh number,  $Ra_c \approx 10^3$ . For a mantle heated entirely from below  $Ra$  is defined by

$$Ra = Ra_E = \frac{\alpha g(T - T_S)D^3}{\kappa\nu} \quad (4)$$

This definition has been used by [13] to study the loss of primordial heat, initially stored in the core, through mantle convection. For a mantle heated entirely from within,  $Ra$  is defined by

$$Ra = Ra_I = \frac{\alpha gQ(R_m - R_c)^5}{\kappa^2\nu\rho c} \quad (5)$$

In (1) the lower boundary of the mantle is explicitly assumed to be insulated, and the second definition of the Rayleigh number,  $Ra_1$ , should be used. However, several authors have used the first definition [10,14–16], based on the claim made in [10] that this was justified if  $T$  in (4) represents the characteristic temperature of the convecting region.

A temperature-dependent rheology of the form

$$\nu = \nu_0 \exp(A/T) \quad (6)$$

has been used in the models. The parameter  $A$  can be interpreted as an activation temperature. Several formulations have been used to determine  $A$ , either using Weertman and Weertman's formulation based on homologous temperature ( $A = \gamma T_m$ ,  $\gamma \approx 30$ ) [17], using activation energy ( $A = E/R$ ), or both activation energy and volume ( $A = (E + pV)/R$ ). Determination of the value of  $A$  to be used in (6) from the formulations mentioned above is correct only for Newtonian fluids. In non-Newtonian fluids the activation temperature decreases by a factor equal to the

power law index  $n$  in comparison to the Newtonian fluid, an effect that has been disregarded by several authors [9,18]. To include the effect of volatiles an effective  $A$  as a function of volatile content has been defined through the melting temperature  $T_m$  [15,18].

The general form of the heat production is

$$Q = Q_0 \exp(-\lambda t) \quad (7)$$

where  $\lambda$  is the decay rate of the radioactive material and  $Q_0$  is the heat production at  $t = 0$ . Jackson and Pollack [15] have used an effective  $\lambda$  to describe a mixture of several isotopes with different decay rates.  $Q_0$  is not well known and in most calculations it has been used as a free parameter;  $Q_0$  was varied to constrain the present-day heat flux at  $70 \text{ mW m}^{-2}$ , based on the estimate of oceanic heat loss [19]. In contrast to this, Sleep [20] and Stacey [21] used the abundance of atmospheric  $^{40}\text{Ar}$  to constrain absolute values of the concentration of  $^{40}\text{K}$  and from that the concentrations of the other heat-producing elements.

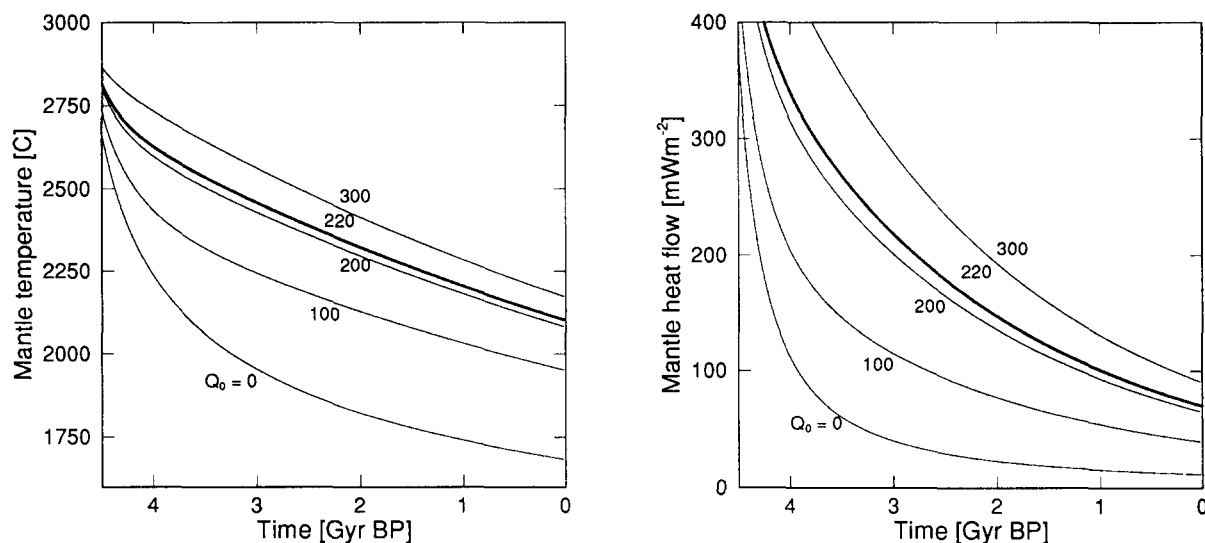


Fig. 1. Example of evolution of internal mantle temperature and surface heat flow, based on parameterised mantle convection modelling (see text). Heat production is given by  $Q(t) = Q_0 \exp(-\lambda t)$ , where the decay constant  $\lambda = 4.48 \cdot 10^{-10} \text{ yr}^{-1}$  is for a chondritic composition [1980]. The initial heat production  $Q_0$  is used as a free parameter.  $Q_0 = 220 \text{ mW} \cdot \text{m}^{-2}$  yields a present-day heat flow of  $70 \text{ mW} \cdot \text{m}^{-2}$ .

Substitution of (2)–(4), (6) and (7) into (1) gives

$$\frac{dT}{dt} = \frac{-3 \left[ \frac{\alpha g (T - T_s) D^3}{Ra_c \kappa \nu_0 \exp(A/T)} \right]^\beta k (T - T_s) R_m^2}{D \rho c_p (R_m^3 - R_c^3)} + \frac{Q_0}{\rho c_p} \exp(-\lambda t) \quad (8)$$

This non-linear differential equation can be solved numerically. A typical result is shown in Fig. 1, which displays the averaged mantle temperature and mantle heat flow as a function of age. A fourth-order Runge–Kutta scheme with a constant step size of 10 Myr has been used to solve (8). The nominal values shown in Table 1 and a decay rate of  $\lambda = 4.48 \times 10^{-10} \text{ yr}^{-1}$  have been used. This decay rate corresponds to the time-averaged decay constant for a chondritic composition [10]. The initial condition is  $T = 3000^\circ\text{C}$ . The model run with  $Q_0 = 220 \text{ mW m}^{-3}$  (bold line) yields a present-day heat flow of  $70 \text{ mW m}^{-2}$ . Other models include different distributions of radioactive heat sources [e.g., 14], volatile-dependent rheology and the de/regassing history of the Earth [16,18]. In general, the results show the strong self-regulating effect of the temperature- and volatile-dependent rheology on the dynamic cooling and a temperature decrease of 200–300 K since the Archaean. A lower estimate of the amount of cooling is made by Davies [9], who derives from isoviscous models that the Earth cannot have cooled by more than 100–150 K since the early Archaean.

The assumptions and simplifications that have been used to make this analysis possible make it difficult to judge the applicability of these models to the evolution of the Earth. One point of criticism applies to the Nusselt–Rayleigh number relation employed, which in general does not take into account the effects of large aspect ratio convection [22], viscous dissipation [23], and depth variations in rheological [24] and thermodynamic properties [25,26].

Another shortcoming of the models concerns the implementation of temperature-dependent rheology, as has been pointed out by Christensen

[27,28], who essentially indicates the importance of the rheology of the upper boundary layer in controlling the cooling of the Earth. As the surface temperature is assumed to have varied very little over geological time, the upper boundary layer may well have a rheology that is largely independent of the internal temperature. A consequence could be that the Nusselt number  $Nu$  would become independent of the Rayleigh number and heat flux would be constant throughout most of the Earth's history. As will be shown later, this effect might be less important for high Rayleigh number ( $Ra < 10^8$ ) convection, for which the heat flow would become a function of  $Ra$  again, even for strongly temperature-dependent viscosity [60]. However, it is not clear if these high Rayleigh number convection results apply to the Earth, even in its early history.

In addition to this, Vlaar [3,11] and Vlaar and Van den Berg [29] have shown that the thicker basaltic and underlying depleted harzburgitic layer, that are created at higher mantle temperatures [20], constitute a compositional boundary layer with a strong stabilizing influence that might effectively prohibit plate tectonics from operating in the way that it does today. This effect has been thus far disregarded.

In order to study the thermal evolution of the Earth since the early Archaean, it is essential to incorporate these rheological and compositional properties of the upper thermal boundary layer. In the present paper we will assume that the cooling of the Earth is completely governed by the dynamics of the upper boundary layer. Any sinking material is passively replaced by adiabatically upwelling mantle. This approach is similar to that of Sleep [20], who used analytical half-space cooling models, combined with estimates of the average age of the oceanic lithosphere, to study the thermal evolution.

### 3. Pressure-release melting

The process of pressure-release melting of un-depleted mantle peridotite plays an important role in the Earth. It is held to be the cause of the

present-day generation of basaltic oceanic crust at mid-ocean ridges. It is generally agreed that in a hotter mantle the melting of a rising diapir starts at a deeper level and a larger volume of basaltic magma is formed [11,20,30,31,61]. McKenzie and Bickle [32] derive the thickness of the formed basaltic crust as a function of the potential temperature of the mantle, which is defined as the temperature obtained when a material volume in the mantle is decompressed under isentropic and metastable conditions to the pressure at the Earth's surface. Estimates for the present-day potential temperature range from 1280 to 1400°C [20,28,30,33]. This range indicates the uncertainties in the eruption temperatures of basaltic magmas, the temperature drop as a consequence of the latent heat consumption, and possible lateral variations in potential temperature [61]. An important effect that has not been implemented by McKenzie and Bickle [32] is that the amount of melting will be influenced by the

pressure that is exerted by the already formed basaltic crust. This will lead to considerably reduced production of basaltic crust upon pressure-release melting [29].

Fig. 2a illustrates the effect of higher mantle temperature on the melting of an adiabatically rising diapir, using the formalism developed by McKenzie [30], corrected for the crustal pressure effect [29]. Shown are the solidus and liquidus of mantle peridotite, each given as a third-order polynomial fit to the data of Takahashi [31],  $T(p) = a_0 + a_1 p^1 + a_2 p^2 + a_3 p^3$ . The coefficients can be written as a vector  $a$ . These are given, with pressure in GPa and temperature in °C, by  $a = (1136, 134.2, -6.581, 0.1054)^T$  for the solidus, and  $a = (1762, 57.46, -3.487, 0.0769)^T$  for the liquidus. In the calculations a small correction is made to account for the fact that Takahashi [31] used a slightly depleted mantle peridotite in his experiments. The dotted lines indicate lines of equal melting for 15 and 50% melting, based on

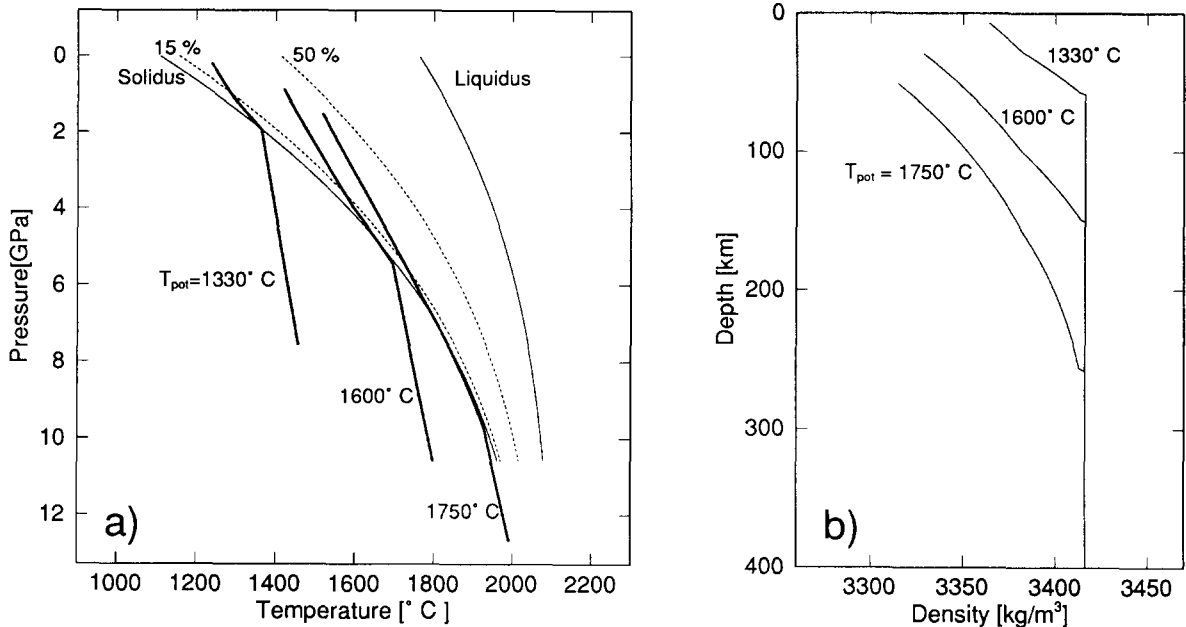


Fig. 2. (a) The effect of higher mantle temperatures on the pressure-release melting of an adiabatically rising diapir. The solidus and liquidus of mantle peridotite are shown as a third-order polynomial fit (see text). Lines of equal melting for 15 and 50% melt fractions are shown, based on the data of Jaques and Green [34]. The heavy solid lines schematically indicate the  $(T, p)$  paths of a rising diapir at potential temperatures  $T_{pot} = 1330, 1600$  and  $1750^\circ\text{C}$ , based on [30]. In the calculations we have corrected for the crustal pressure effect [29] (see text). (b) Compositional density in harzburgite and lherzolite. Density increases with depth, as a consequence of the lower degree of depletion.

data from Jaques and Green [34]. For the entropy of melting, we used  $\Delta S = 300 \text{ J} \cdot \text{kg}^{-1} \text{ K}^{-1}$ , which is approximately equivalent to  $1 R \text{ J} \cdot \text{mol}(\text{atom})^{-1} \text{ K}^{-1}$  [35,36]. The bold lines indicate the  $(T, p)$  paths for rising diapirs at three different potential temperatures,  $T_{\text{pot}} = 1330, 1600$  and  $1750^\circ\text{C}$ . The present-day situation, with a crustal thickness of 7 km, is simulated with  $T_{\text{pot}} = 1330^\circ\text{C}$ . The extrusion temperature here is  $T_{\text{extr}} = 1240^\circ\text{C}$ . At  $T_{\text{pot}} = 1600^\circ\text{C}$ , 29 km of basaltic crust is generated with  $T_{\text{extr}} = 1420^\circ\text{C}$ . At the highest potential temperature shown,  $T_{\text{pot}} = 1750^\circ\text{C}$ , melting of a rising diapir generates 50 km of basaltic crust with  $T_{\text{extr}} = 1520^\circ\text{C}$ . In general, it is stated that the decrease in temperature indicates heat loss by the consumption of latent heat. Strictly speaking, however, this is not correct. Pressure-release melting occurs in adiabatically rising mantle material and no heat is lost from the system. The temperature decreases to account for the entropy increase of the melt fraction. Only when the melt reaches the surface and solidifies is heat lost by the entropy decrease. However, we will assume that the amount of heat lost by the melt fraction at the surface equals the heat necessary to melt the peridotite at depth.

Note the strong effect of the consumption of latent heat on the extrusion temperatures. Although the potential temperatures differ by  $420^\circ\text{C}$ , the temperatures at the 50 km depth differ by only  $280^\circ\text{C}$ . This important effect should be taken into account when using estimates of extrusion temperature to constrain the potential mantle temperature.

Fig. 2b shows the density in the underlying depleted harzburgitic residue for the three cases with different potential temperature. The density of the harzburgite increases with depth as a consequence of the decreasing amount of depletion. As has been shown by Vlaar [11] and Vlaar and Van den Berg [29], this compositional basalt–harzburgite stratification has a large effect on the stability of the oceanic lithosphere.

In this scenario, komatiite might be the melt generated at considerable depth ( $> 150 \text{ km}$ ) and at low degrees of partial melting in a rising diapir. At depth, the komatiitic magma separates from the matrix and rises adiabatically to the

surface [5,31,37]. In time, this is followed by the more basaltic outflows from the diapir, caused by pressure-release melting and, consequently, much lower extrusion temperatures. This can explain the occurrence of high-temperature komatiites as the first extrusion product in greenstone belt formation, followed by outflows of less MgO-rich basaltic lavas [38].

In the following section we will discuss the consequences of the aforementioned effects for the dynamics of the lithosphere in a hotter mantle.

#### 4. Consequences for upper mantle dynamics

Vlaar [3,11] presented qualitative constraints on Archaean global dynamics; these are summarised as follows:

- (i) The mantle was originally molten shortly after accretion [39].
- (ii) Rapid solidification started at the bottom of the mantle and progressed upward [36] until the whole mantle was at or below the solidus temperature.
- (iii) At high mantle temperatures, pressure-release melting of rising diapirs generates a thick basaltic layer on top of a very thick harzburgitic layer [11,20,32].
- (iv) Compositional stability [40–42] and lack of mechanical coherency of this upper boundary layer [43] renders modern-style plate tectonics ineffective [3,11].
- (v) Continents stabilised on top of strong chemical zonation in the harzburgitic root and the generation of radiogenic heat in the continental crust blankets the surface cooling [11].
- (vi) After formation of stable basalt–harzburgite layering, recycling of basaltic material can occur through its denser phases (garnet–granulite and eclogite). The recycling of eclogite allows for new generation of basaltic magma.

In the following section we will consider the consequences of these assumptions and constraints on the evolution of the lithosphere and upper mantle in a hotter Earth.

## 5. Dynamic modelling

### 5.1. Model description

We have employed a two-dimensional thermochemical model of the cooling of the lithosphere and upper mantle (to a depth of 400 km), both in an oceanic and continental setting. This is schematically indicated in Fig. 3. In the continental model (Fig. 3a) a crust of 50 km in thickness (consisting of a 10 km thick granitic upper crust on top of a 40 km thick more tonalitic or granulitic lower crust) overlies a thick harzburgitic root. The radioactive heat production is indicated too in Fig. 3a. The value of the upper crust is based on the estimate for the heat production of a young surface shield [44], corrected for the assumed  $3 \times$  higher productivity in the early Earth. The lower crust is assumed to have a  $10 \times$  lower heat production. The oceanic lithosphere/upper mantle (Fig. 3b) comprises the layering formed through decompression melting of rising diapirs, with basalt (B) on top of depleted peridotite (harzburgite, Hz), overlying the undepleted mantle peridotite (lherzolite, Lh). The harzburgite layer has a density gradient as a consequence of the varying degree of depletion by partial melting with depth. The properties of the layering are strongly dependent on potential mantle temperature.

The stability of these models against cooling from the top is considered. The free-slip upper

boundary is kept at constant temperature  $T = 0^\circ\text{C}$ . At the lower boundary a constant, adiabatic temperature gradient is maintained.

To describe the rheology of the lithosphere and mantle we have used linearised ductile creep laws, following [43]. The general form of the creep law is given by

$$\sigma = (\dot{\epsilon}/B)^{1/n} \exp(E/nRT) \quad (9)$$

where  $\sigma$  is differential stress (MPa),  $\dot{\epsilon}$  the strain rate ( $\text{s}^{-1}$ ),  $n$  the power law index,  $E$  the activation energy ( $\text{J mol}^{-1} \text{K}^{-1}$ ),  $R$  the gas constant ( $8.314 \text{ J mol}^{-1}$ ),  $T$  the absolute temperature (K), and  $B$  a constitutive parameter. Note that  $\sigma$  here is specified in MPa. From this we can derive an effective viscosity  $\eta = \sigma/2\dot{\epsilon}$  ( $\text{MPa} \cdot \text{s}$ ), which can be expressed as

$$\eta = C \exp(E/nRT) \quad (10)$$

where

$$C = \frac{10^6}{2} \cdot \left[ \frac{\dot{\epsilon}^{1-n}}{B} \right]^{1/n} \quad (\text{Pa} \cdot \text{s}) \quad (11)$$

The numerical values for diabase have been used to model basalt and eclogite, the values for peridotite have been used to model harzburgite and lherzolite. Table 2 gives the values for  $B$ ,  $n$  and  $E$  from [43] and the value of  $C$  for  $\dot{\epsilon} = 10^{-15} \text{ s}^{-1}$ . Fig. 4 shows the effective viscosity of diabase and peridotite as a function of temperature.

#### (a) Continental lithosphere

10 km	upper crust	$A=7500 \text{ nW/m}^3$
40 km	lower crust	$A=750 \text{ nW/m}^3$
		$\rho=3.315 \text{ g/cm}^3$
	harzburgite	
		$\rho=3.416 \text{ g/cm}^3$
50 km	lherzolite	$\rho=3.416 \text{ g/cm}^3$

#### (b) Oceanic lithosphere

30–50 km	basalt	$\rho=3.0 \text{ g/cm}^3$
		$\rho=3.315 \text{ g/cm}^3$
	harzburgite	
		$\rho=3.416 \text{ g/cm}^3$
250 km	lherzolite	$\rho=3.416 \text{ g/cm}^3$

Fig. 3. Schematic overview of the compositional layering for the (a) continental and (b) oceanic lithosphere–upper mantle in a “hot Earth”, with potential temperatures  $T_{\text{pot}} > 1600^\circ\text{C}$ .

Table 2  
Parameters used in the rheological description (11)

Rock	$\log B$ (MPa <sup>-n</sup> s <sup>-1</sup> )	$n$	$E$ (kJmol <sup>-1</sup> )	$C$ (Pa · s)
Diabase	-2.5	3.3	268	$81 \times 10^{15}$
Peridotite	4.5	3.6	535	$19 \times 10^{14}$

The equations governing the models are the Stokes equation together with the incompressibility constraint, the advection–diffusion equation for temperature and the advection equation for the composition [e.g., 46,47]. The equations are solved numerically by finite-element methods. The Stokes equation is solved in the stream function formulation, using a non-conforming type of element [22,45,46]. The time-dependent heat equation is solved using linear triangles and a predictor–corrector method. The Boussinesq approximation is used and the adiabatic temperature increase with depth has no influence on the dynamics of the model. In the numerical model this adiabatic temperature difference is subtracted from the absolute temperature. The absolute temperature is used in the calculation of viscosity and for output purposes. For the advection equation for the composition we have used a mixed approach. The discontinuous density jumps, as for example between the basalt and harzburgite (Fig. 2b) are modelled using a marker

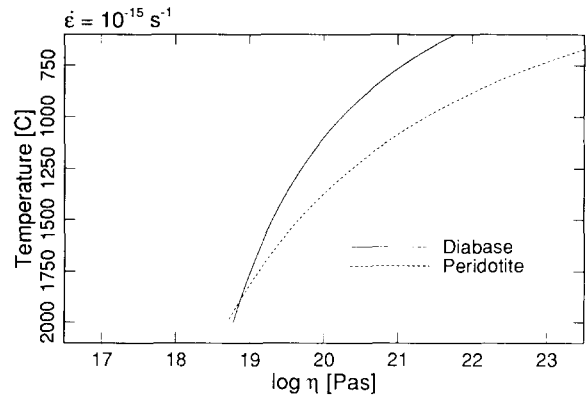


Fig. 4. Effective viscosity of diabase (used to model basalt and eclogite) and peridotite (used to model harzburgite and lherzolite) as a function of temperature. Rheological parameters are defined in Table 2.

chain method [e.g., 46,47]. The density gradient in the harzburgite is modelled using a field approach. The time step in the predictor–corrector method was taken as 50% of the Courant time step with an upper limit of 1 Myr.

## 5.2. Results

### Continental lithosphere, potential temperature 1750°C

The evolution of the continental lithosphere is shown in Fig. 5. The lower crust is slightly thicker

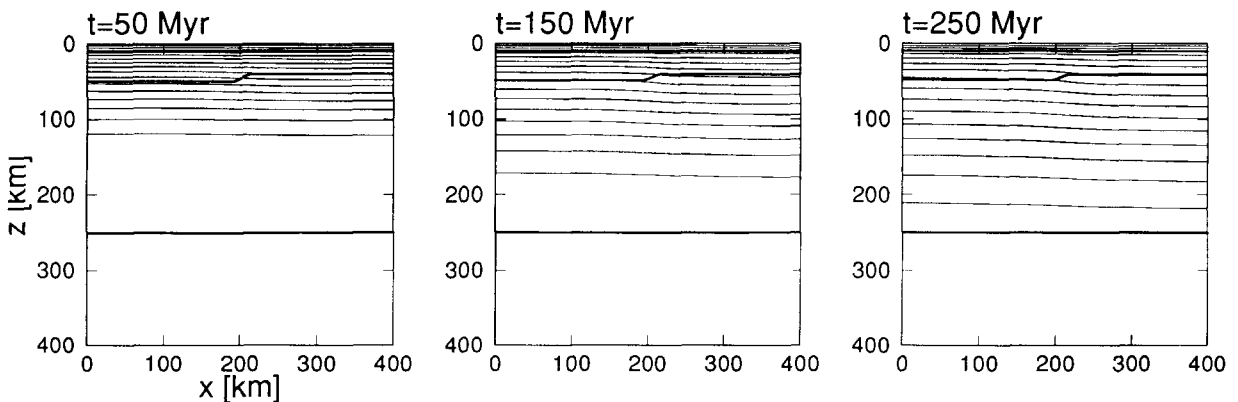


Fig. 5. Evolution of a cooling continental lithosphere. The compositional stratification and distribution of heat-producing elements are defined in Fig. 3. Retarded by the crustal heat production, the cooling progresses slowly to deeper levels. As a consequence of the density gradient in the harzburgitic root, the lithosphere remains stably stratified.

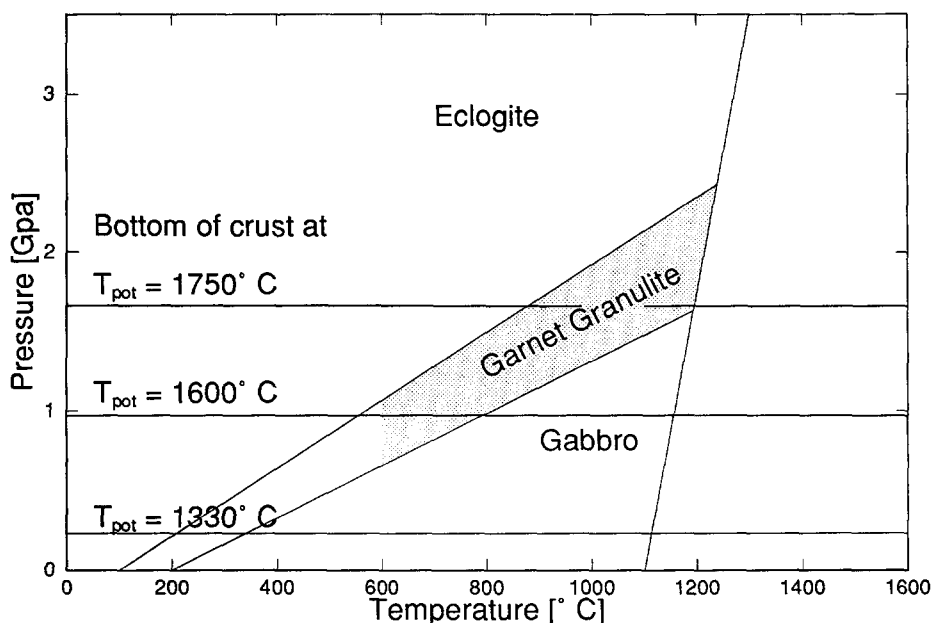


Fig. 6. Phase diagram for basalt [48].

on one side of the model, to avoid the model remaining artificially stably stratified. The first frame shows the initial temperature profile, based

on the  $(T, p)$  path of a rising diapir. The crustal heat production balances ('blankets') only partially the heat loss through the top and the cool-

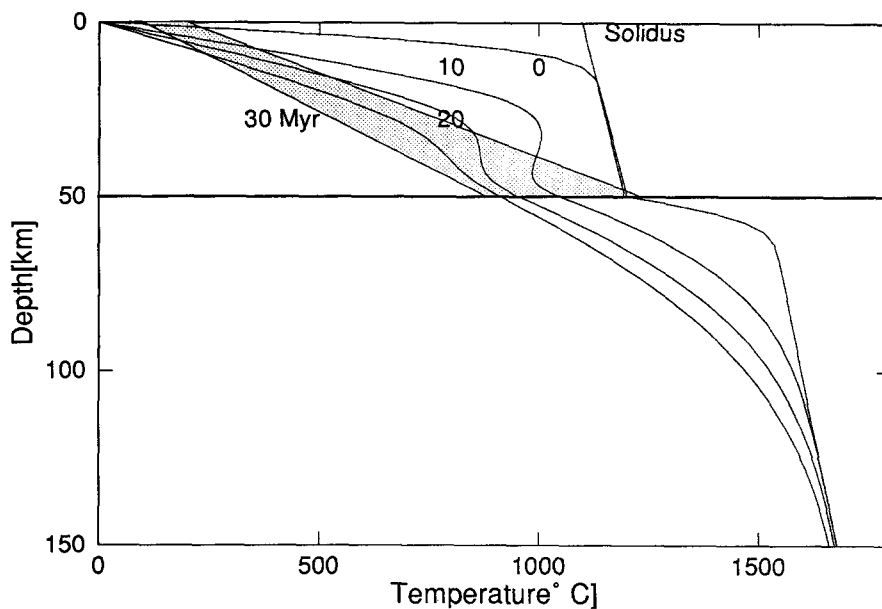


Fig. 7. Evolution of the horizontally averaged temperature in the oceanic lithosphere generated at  $T = 1750^{\circ}\text{C}$ . Convection in the basalt generates an asthenosphere and relatively cool temperatures in the lower crust.

ing progresses slowly to larger depths. As is shown in Fig. 5, the continental lithosphere is stable to at least 250 Myr. After this, the cooling progresses into the undepleted peridotitic layer. In some simulations this creates an instability in the lower parts of the model, which can recycle the lower most parts of the (now thermally defined) continental root. However, the most important result of these simulations is that the proposed layering is intrinsically stable to cooling. This leads to a firm basis for the suggestion that the early protocontinents were able to resist recycling on top of a chemically zoned root, and that the present thickness of the continental cratons (ca. 200 km) has been maintained throughout geological history.

#### *Oceanic lithosphere, potential temperature 1750°C*

The oceanic lithosphere, formed at  $T_{\text{pot}} = 1750^\circ\text{C}$ , is stably stratified in a fashion similar to that of the continental lithosphere discussed above. Recycling of the basaltic crust and underlying harzburgite can only be achieved in this environment through the formation of the denser phases of gabbroic basalt: garnet-granulite (GG,  $\rho \approx 3.3 \text{ g} \cdot \text{cm}^{-3}$ ) and eclogite (E,  $\rho \approx 3.6 \text{ g} \cdot \text{cm}^{-3}$ ). Fig. 6 shows a phase diagram for basalt taken from [48]. The horizontal lines indicate the pressures at the base of the crust, formed at  $T_{\text{pot}} = 1750, 1600$  and  $1330^\circ\text{C}$  respectively. At  $T_{\text{pot}} = 1750^\circ\text{C}$ , the crust is approximately 50 km thick and solid-state convection can occur in the basaltic layer (assuming that the upper brittle crust has negligible influence on the dynamics). Fig. 7 shows the evolution of the horizontally averaged temperature in the oceanic lithosphere. The initial temperature profile beneath the basalt layer is taken from Fig. 2a. It is assumed that after formation the basaltic crust solidified very rapidly and that the basalt is at its solidus temperature, except for the thin boundary layer on top. The grey area indicates the garnet-granulite stability field, taken from Fig. 6. Cooling progresses rapidly through the efficient heat loss by the combined effects of conduction and low Rayleigh number convection. After 10 Myr, the lower part of the crust is in the garnet-granulite stability field. Garnet-granulite is nearly as dense

as the underlying harzburgite. The cooler garnet-granulite may have a density that is high enough to recycle into the mantle, although the density difference with the underlying harzburgite is not very large. A more efficient way of recycling the basaltic crust is through its high-density phase eclogite. This is considered in the following paragraphs.

Just after it forms the brittle layer is thin and weak [43], and can probably not resist sinking into the hot ductile lower crust. Through this mechanism of crustal, or 'mini'-subduction, a relatively cool ( $T < 1000^\circ\text{C}$ ) and hydrated basaltic layer can be formed on top of the harzburgite. Under these conditions, the transformation from gabbro to eclogite is fast, with time scales of the order of 1 Myr [49]. Once eclogite is formed, recycling of crustal material into the harzburgitic layer is fast. Fig. 8 illustrates this for a layering formed at potential temperature  $T_{\text{pot}} = 1750^\circ\text{C}$ . The eclogite layer is 10 km thick and within 5 Myr most of the eclogite is recycled into the underlying harzburgite.

#### *Oceanic lithosphere, potential temperature 1600°C*

At lower potential temperature, the recycling of eclogite will become less efficient, and eventually cease. The viscosity of the lower basaltic crust and harzburgite increases, the recycling of hydrated crust will become less efficient and eclogitisation is less rapid. The less efficient eclogitisation of the lower crust is the main factor determining the lower speed of the mechanism. The increase in viscosity and thinning of the eclogite layer have only a minor effect, as is illustrated in Fig. 9, where the recycling of a now 5 km thick eclogitic layer is shown in a model based on a basalt-harzburgite layering formed at  $T_{\text{pot}} = 1600^\circ\text{C}$ . The basaltic crust has a total thickness of 29 km. Initial temperature and compositional density are given for the harzburgite/lherzolite in Fig. 2a and b. Recycling of the eclogite layer is now approximately  $2 \times$  slower.

At even lower temperatures the crust will become too thin and the brittle upper crust too strong for crustal subduction to take place and pressures at the bottom of the crust may be too low for eclogite to be formed, although it is not

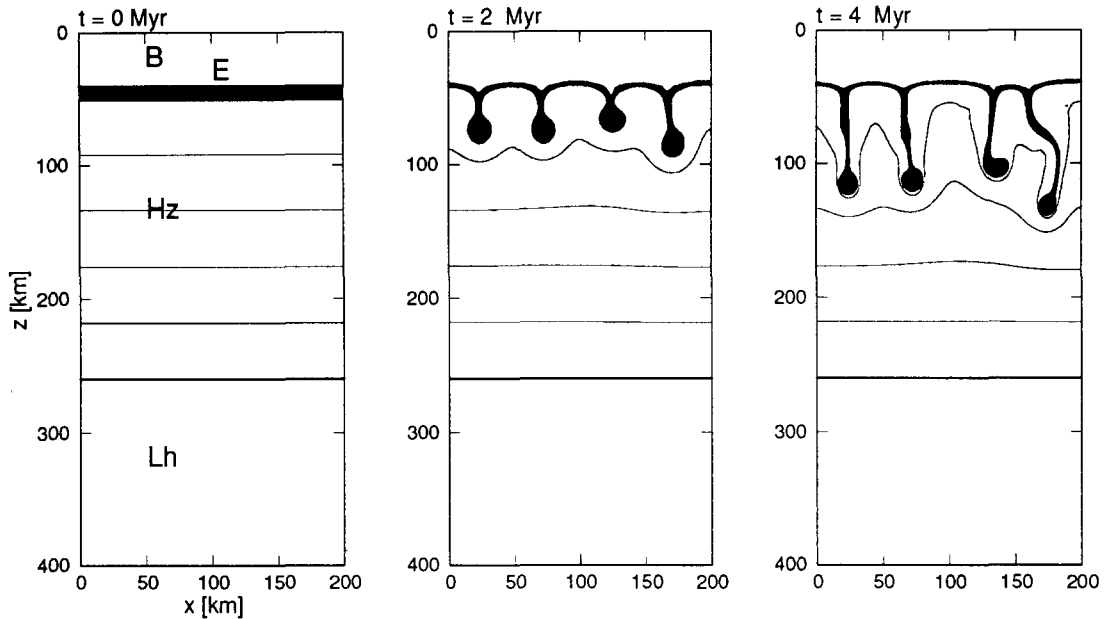


Fig. 8. The recycling of eclogite into the upper mantle. Original oceanic lithosphere generated at 1750°C.

clear at which crustal thickness this will occur. The phase diagram for basalt shown in Fig. 6 indicates that eclogite cannot be formed at crustal thicknesses of less than ca. 25 km. However,

some evidence exists for the formation of eclogite from hydrated basalt at the shallower levels [49]. The driving forces of the present-day form of plate tectonics will become increasingly impor-

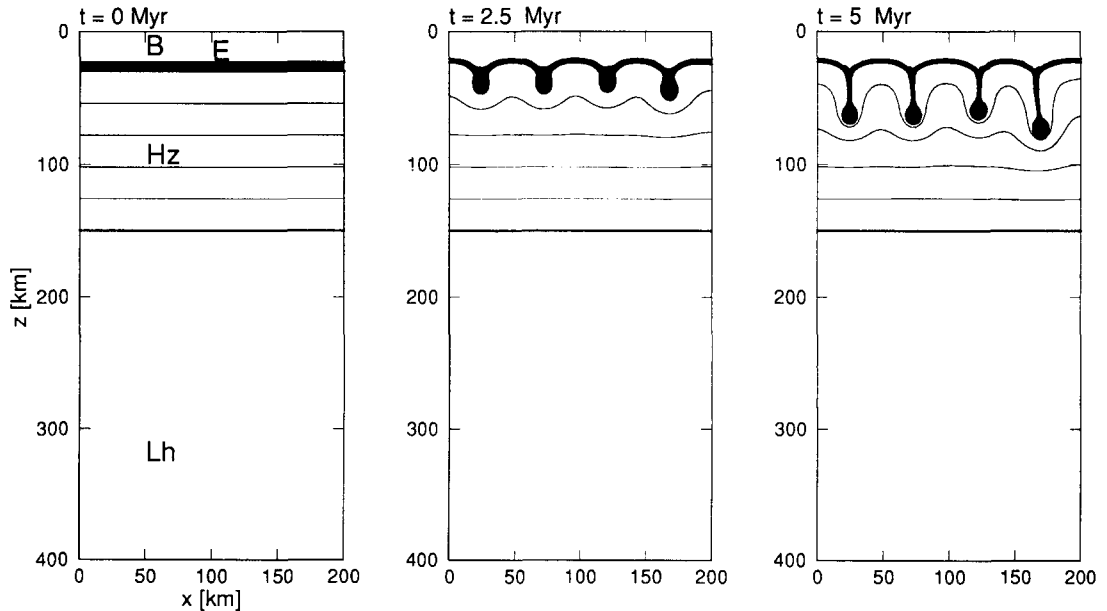


Fig. 9. The recycling of eclogite into the upper mantle. Original oceanic lithosphere generated at 1600°C.

tant and in a certain temperature range a gradual transition from the proposed mechanism and plate tectonics may occur. We tentatively place this transition at a potential ‘blocking’ temperature of  $T_{\text{pot}} = T_0 = 1475^\circ\text{C}$ , at which 15 km of crust is produced.

#### *Consequences of eclogite recycling*

The models presented above indicate the time the eclogite can reside in the lower crust and an eclogite recycling rate can be estimated. Once the eclogite starts sinking into the underlying harzburgite, several processes can be envisaged. Firstly, the eclogite will heat up (see Fig. 7) and will melt once its temperature is above the solidus, leading to new creation of basalt and tonalite. Secondly, the uppermost parts of the harzburgitic layer will be entrained by the sinking eclogite, which will lead to passive upwelling of the harzburgite, and, if the top of the harzburgite is still hot enough, some new basalt can be formed by pressure-release melting. If this process continues for some time, further depletion of the harzburgitic layer might result: depleted harzburgite is recycled into the underlying less depleted layers, which eventually may lead to homogenisation of part of the harzburgitic layer in which thermal convection can lead to rapid cooling. This in turn may trigger an overturn of the basalt–harzburgite system, generating renewed pressure-release melting. Lastly, thinning of the eclogite and mixing into the harzburgite may lead to enrichment of the harzburgite, but the reaction time is expected to be long, and the volumes involved relatively small. Implicitly, this scenario assumes that when the mantle temperature is constant the thickness of the basaltic crust remains constant. Thinning of the basaltic crust is assumed to occur only when the potential mantle temperature decreases.

Because of the different time scales and the complex interaction between the mechanisms the interaction between them is extremely difficult to model. We choose to simplify the model description by assuming that we can describe the processes above by a continuous model in which it is assumed that the eclogite layer is recycled in the mantle and completely replaced at crustal levels

by new basalt which is either generated by eclogite remelting or pressure-release melting of harzburgite. Using this simplifying description, we propose that this mechanism of recycling of basaltic crust through mini-subduction, rapid eclogitisation at the bottom of the crust, recycling of the eclogite into the upper mantle and formation of new crust is responsible for the initial cooling of the hot Earth, after solidification of the mantle, but will grow less efficient in the cooling Earth. We take the rate of eclogite recycling, that can be estimated from the model results presented above, to be the factor governing the rate of cooling induced by the present scenario. Both the formation of eclogite from hydrated basaltic crust and remelting of the eclogite are assumed to occur at shorter time scales.

## **6. A thermal model for the early Earth**

We will now turn to the consequences of the presented dynamic model for the thermal history of the Earth. Our approach to this problem is necessarily conjectural, due to the lack of detailed knowledge of the interaction between the different processes and the variability of the parameters governing the dynamic behaviour.

We assume that the cooling of the Earth’s mantle is entirely caused by heat loss through the oceanic lithosphere. This is presently estimated at  $3 \times 10^{13}$  W, predominantly (> 90%) by the conductive cooling of the continuously recycling lithosphere [19]. The consumption of latent heat at mid-oceanic ridges is only a fraction of this [31]. However, in a hotter mantle, the amount of melt generated is much larger and the dissipation of heat by solidification of extruding magma may be the dominant form of cooling of the Earth [31,50]. We will use this and estimate the amount of cooling in our models by (i) advection of magma to the surface, (ii) consumption of latent heat by solidification of magma and remelting of eclogite, and (iii) conductive cooling of the basaltic crust. The key parameter is the rate of recycling of basaltic crust through the eclogite phase. We will make some simplifying assumptions regarding the recycling process. Recycling of the eclogitic layer

will result in at least partial remelting of the eclogite in the underlying mantle. Suppose a fraction  $b$  of the eclogite remelts. The melting of this eclogite will consume an amount of latent heat  $b\rho L\dot{V}$ . We can only guess at the numerical value of this fraction  $b$ , which depends on details of the eclogite recycling process and the ambient temperature. We tentatively put this value at  $b = 0.5$ . The formed melt migrates through the harzburgite and forms new crust. At the same time, the harzburgitic root will move upward to fill in the gap left by the removed eclogite. We will assume that the combined effect of remelting of eclogite and renewed pressure-release melting leads to a complete replacement of the removed eclogite by new basaltic crust. The amount of latent heat released upon solidification of this new basaltic crust is equal to  $\rho L\dot{V}$ , where  $\rho = 3000 \text{ kg} \cdot \text{m}^{-3}$  is the density,  $L = 6 \times 10^5 \text{ J kg}^{-1}$  the latent heat of basalt melt [51], and  $\dot{V}$  the rate of eclogite recycling (in  $\text{m}^3 \cdot \text{s}^{-1}$ ). The maximum total heat consumption through latent heat effects is thus  $(1 + b)\rho L\dot{V}$ . The basaltic magma is generated at a specific extrusion temperature  $T_{\text{extr}}$ . Percolation of magma to the surface will continue until the temperature in the basaltic layer is below the solidus temperature, leading to additional heat loss, estimated at  $\rho c_p \dot{V}(T_{\text{extr}} - T_{\text{SB}})$ , where  $c_p = 1.3 \times 10^3 \text{ J kg}^{-1} \text{ K}^{-1}$  is the specific heat and  $T_{\text{SB}} = 1200^\circ\text{C}$  is the solidus temperature of basalt (assumed constant here). This simple linear relationship is chosen because of a lack of knowledge of better parameterisation. Furthermore, we will assume that the process of eclogite recycling is continuous and that this process leads to a continuous decrease in mantle temperature. The amount of crustal recycling is strongly dependent on potential temperature, through the processes described above. We will parameterise this influence as a linear function  $\dot{V} = a(T_{\text{pot}} - T_0)$ , where  $T_0$  is the previously defined blocking temperature. The parameter  $a$  depends on the rates of crustal subduction, eclogite formation and eclogite recycling. The maximum combined rate is determined by the recycling rate of eclogite, which can be estimated from the results above to be approximately  $5 \text{ km} \cdot \text{Myr}^{-1}$  at  $T_{\text{pot}} = 1750^\circ\text{C}$ . Assuming that 70% of the Earth's surface is oceanic,

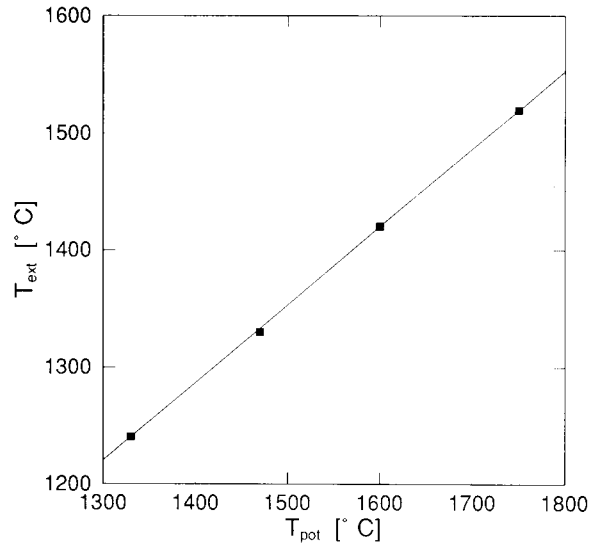


Fig. 10. Dependence of extrusion temperature  $T_{\text{extr}}$  on the potential temperature  $T_{\text{pot}}$ . Points indicate the calculations made using the formalism of McKenzie [5], corrected for the crustal pressure effect [29]. The solid line indicates the first-order approximation  $T_{\text{extr}} = 2/3 \times (T_{\text{pot}} - 1330) + 1240^\circ\text{C}$ .

we can convert this to an effective rate

$$\begin{aligned} \dot{V}_{\text{max}} &= (5 \text{ km} \cdot \text{Myr}^{-1}) \times (0.7 \times 5 \times 10^8 \text{ km}^2) \\ &= 1.8 \times 10^9 \text{ km}^3 \text{ Myr}^{-1} \end{aligned} \quad (12a)$$

with corresponding

$$a_{\text{max}} = 6.4 \times 10^6 \text{ km}^3 \text{ Myr}^{-1} \text{ K}^{-1} \quad (12b)$$

The extrusion temperature  $T_{\text{extr}}$  depends on the potential temperature as well. In a first-order approximation this dependence is given by (Fig. 10):

$$T_{\text{extr}} = 2/3 \times (T_{\text{pot}} - 1330) + 1240^\circ\text{C} \quad (13)$$

In this model, we can only guess at the rate of cooling through conductive heat loss. The dynamic models presented above indicate only the efficiency of eclogite recycling, once it is formed. The model in Eq. (11) does not provide us with information on the processes controlling melt segregation, melt migration and the temperature distribution in the lithospheric column as has been described above. We estimate that, compared to heat loss by melt migration and solidification, conductive cooling makes only a minor

contribution to the total heat loss in the hotter Earth. For all practical purposes we assume that the conductive heat loss has not varied through geological time, and fix it at the present-day value of

$$4\pi qR_m^2 = 3 \times 10^{13} \text{ W} \quad (14a)$$

In comparison, at the highest estimated recycling rate  $\dot{V}_{\max}$ , the cooling through melt solidification, assumed equal to the latent heat consumption, contributes

$$\rho L \dot{V}_{\max} = 2 \times 10^{14} \text{ W} \quad (14b)$$

and the melt migration contributes ( $T_{\text{pot}} = 1750^\circ\text{C}$ )

$$\rho c_p (T_{\text{extr}} - T_{\text{SB}}) \dot{V}_m a_x = 1.5 \times 10^{14} \text{ W} \quad (14c)$$

We can now model the thermal evolution of the Earth using an extension to (1), given

$$\begin{aligned} & \frac{4\pi}{3} \rho c_p (R_m^3 - R_c^3) \frac{dT}{dt} \\ &= -4\pi q R_m^2 + \frac{4\pi}{3} Q (R_m^3 - R_c^3) \\ & \quad - \rho c_p \dot{V} (T_{\text{extr}} - T_{\text{SB}}) - (1+b) \rho L \dot{V} \end{aligned} \quad (15)$$

The temperature  $T$  is the mean mantle temperature, which is assumed to be the temperature at a depth of 1500 km. The relationship with the potential temperature is given as  $T = T_{\text{pot}} + 750$ , assuming a constant adiabatic gradient of  $0.5 \text{ K} \cdot \text{km}^{-1}$ . Heat production  $Q$  is modelled using

Sleep's estimates of the absolute mantle abundance of K, U and Th from the amount of  $^{40}\text{Ar}$  [20]. Fig. 11 shows the evolution of the model, initially with  $T_{\text{pot}} = 1750^\circ\text{C}$  for initial crustal recycling rates of  $0.5\dot{V}_{\max}$ ,  $0.2\dot{V}_{\max}$  and  $0.1\dot{V}_{\max}$ . Note that the dimensional time shown on the horizontal axis indicates the time that has elapsed since the calculation started. It does not necessarily coincide with the age of the Earth. Shown are, from left to right, the potential temperature  $T_{\text{pot}}$  ( $^\circ\text{C}$ ) and latent heat consumption and heat advected by migrating melt (both in  $10^{12} \text{ W}$ ). At potential temperature  $T_0 = 1475^\circ\text{C}$ , it is assumed that the mechanism becomes inefficient and heat loss is governed by conductive heat loss (14a) only. At the highest recycling rate shown the Earth cools by more than 200 K within 200 Myr. At  $t = 0.5 \text{ Gyr}$ , the blocking temperature  $T_0$  is reached. At the lower recycling rates the cooling progresses slower, but still a large drop in temperature is observed in 1 Gyr. These results should be considered with proper caution as they are based on a rather speculative quantification and error margins are large. Most likely the conductive heat loss has been larger than modelled here, leading to more efficient cooling. The estimates for the radiogenic heat production [20] are rather low compared to others. Increasing the heat production by a factor of 2 leads to much longer cooling times. However, it is not entirely unreasonable to assume that, after the proposed mechanism has been active at some time in the

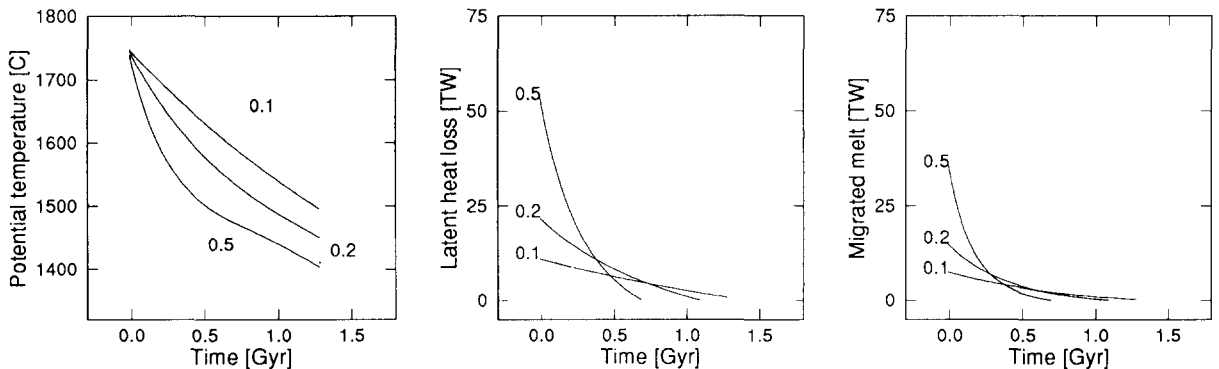


Fig. 11. Influence of the latent heat loss and melt migration on the internal temperature of the Earth (15). Numbers indicate the crustal recycling rate at the arbitrary starting point, put at  $t = 0$ , relative to the proposed maximum  $\dot{V}_{\max}$  (12a).

Earth's history, it has efficiently cooled the mantle by several hundreds of degrees in, say, a 500 Myr period, leading to a moderate mantle temperature that is perhaps 100–200 K higher than the present-day temperature.

Geological constraints on the thermal development of the upper mantle are given by the extrusion temperatures of volcanic rocks. Komatiites indicate the highest mantle temperatures (ca.  $T_{\text{pot}} = 1650\text{--}1750^\circ\text{C}$  at 3.5 Gyr B.P., and  $T_{\text{pot}} = 1500\text{--}1600^\circ\text{C}$  at 2.7 Gyr B.P.). These values are based on the estimates of the extrusion temperatures of komatiites [e.g., 52] and *ad hoc* estimates of the temperature decrease by the consumption of latent heat necessary to generate komatiitic melt at depth, which range from  $0^\circ\text{C}$  [5,31] to  $100^\circ\text{C}$  [20]. Other Archaean volcanic rocks, such as greenstones, have extrusion temperatures that are distinctly lower. Abbott et al. [33] concluded that the mean extrusion temperature determined for such rocks has decreased by approximately 150 K since the middle Archaean (3.0 Gyr B.P.). Note that this is not at odds with the estimated extrusion temperatures estimated for komatiites, which are generated at depth and ascend adiabatically, in contrast to the basaltic outflows found in greenstone belts, which are generated by pressure-release melting. Taking into account the concomitant temperature drop, a decrease in potential mantle temperature of some 250 K can be inferred from the greenstone extrusion temperatures. Therefore, it is not unreasonable to assume that the mean Archaean mantle temperature has been some 200–300 K higher than the present-day temperature. Even higher mantle temperatures imply conditions that are more favourable for eclogite formation and recycling as a consequence of the thicker basaltic layer, lack of mechanical coherency and greater mobility of the crust and upper mantle. The remelting of eclogite upon recycling at moderate depths (50–100 km, see Fig. 7) may well have been important in the formation of tonalitic protocontinents in the very early Archaean [53]. The middle to late Archaean could have been characterised by some form of 'flake tectonics' [43] at the transition between hot Earth dynamics and the present-day plate tectonics. At these moderately higher upper mantle

temperatures, the basaltic crust is still thick enough to resist lithospheric subduction, but is probably too thin to allow efficient eclogite formation and recycling.

## 7. Discussion

In the above, we have illustrated, quantitatively, some dynamic effects that can occur in a hotter mantle. Using the results of the dynamic modelling we can envisage strong episodic behaviour of the upper boundary layer, with periods of relative stabilisation and conductive cooling followed by strong magmatic activity as a consequence of the thermal and compositional instability of the lower basaltic crust and underlying harzburgite.

The interaction between the different mechanisms has yet to be explored, and at present further progress is hampered by technical difficulties: high resolution both in time and space is necessary to resolve the complex interaction. A large problem is presented by the different time scales at which relevant processes take place, as for example the migration of magma compared to the deformation of the solid phase. Studying one of these processes necessitates simplifying assumptions for the other, whereas the two processes are dependent on each other.

### 7.1. Comments on rheological parameters and composition of the crustal layer

The rate of recycling is strongly dependent on the rheology of the basalt/eclogite and harzburgite. Some field evidence exists that eclogite has a lower viscosity than basalt [54]. We have taken this into account in some model calculations but no large difference was observed: as harzburgite is more viscous than both basalt and eclogite at the ambient temperatures (Fig. 4), it controls the speed of the sinking eclogite. In some models we have included pressure dependence by extending the Arrhenius term in (9):  $\sigma \sim \exp [(E + pV)/nRT]$ , where  $p$  is the pressure and  $V$  the activation volume, which was assumed constant ( $V = 10 \text{ cm}^3 \text{ mol}^{-1}$ ). Pressure dependence is rela-

tively unimportant in the upper 100 km and, consequently, little influence on the dynamics could be observed. The linearisation of the power-law creep law (9) will not be correct for strain rates much higher or lower than  $\dot{\epsilon} = 10^{-15} \text{ s}^{-1}$ . In the highest temperature models the recycling of eclogite took place at strain rates significantly higher than this. The non-Newtonian effects will help drain the eclogitic layer even faster.

The crustal layer that is formed by pressure-release melting in a hotter mantle will have a composition that is more komatiitic than that of the present day, and will be slightly denser. This will help to destabilize the compositional layering earlier and the scenario shown above, in which a basaltic composition was assumed for the crust, can be seen as a ‘worst case’ scenario.

### 7.2. Coupling between upper and lower mantle

In the model presented above, we assumed that the cooling of the Earth was completely governed by the dynamics of the upper boundary layer and that any sinking material is replaced by passively upwelling mantle material. This is probably too simple a viewpoint, considering the mounting evidence for the strong influence of the transition zone on mantle dynamics. In recent modelling it has been shown that the thermodynamical [47,55,56,62], compositional [57,58] and rheological [59] properties of the transition zone will retard the exchange of material between the upper and lower mantle. One can envisage a scenario in which the upper mantle is efficiently cooled on top of a temporarily insulated lower mantle, until the temperature difference between upper and lower mantle is sufficiently large to overcome the resistance of the transition zone and large parts of the cold upper mantle are replaced by hot lower mantle. This mechanism may have occurred periodically through geological time.

## 8. Conclusions

We have investigated some aspects of the dynamic behaviour of a mechanism proposed to

cool the Earth in the Archaean. This mechanism involves thermal and compositional advection in a strongly stratified oceanic lithosphere at high average mantle temperatures. The basaltic crust is recycled into the mantle through its high-pressure phase eclogite, leading to renewed pressure-release melting and basaltic crust formation. Consumption of latent heat upon solidification of the melt and the advective cooling through magma migration is sufficient to cool the mantle in the early Archaean by several hundred degrees.

## Acknowledgements

We thank the Dr Schürmann Foundation for generous financial support. We also thank Youxue Zhang and David Yuen for constructive reviews.

## References

- [1] N.H. Sleep, Thermal history and degassing of the earth: some simple calculations, *J. Geol.* 87, 671–686, 1979.
- [2] E.G. Nisbet and C.M.R. Fowler, Model for Archaean plate tectonics, *Geology* 11, 376–379, 1983.
- [3] N.J. Vlaar, Archaean global dynamics, *Geol. Mijnbouw* 65, 91–101, 1986.
- [4] N. Sleep and B.F. Windley, Archean plate tectonics: constraints and inferences, *J. Geol.* 90, 367–379, 1982.
- [5] D.P. McKenzie, The generation and compaction of partially molten rock, *J. Petrol.* 25, 713–765, 1984.
- [6] R. Jeanloz and S. Morris, Temperature distribution in the crust and mantle, *Annu. Rev. Earth Planet. Sci.* 14, 377–415, 1986.
- [7] I.H. Campbell and R.W. Griffiths, The changing nature of mantle hotspots through time: implications for the chemical evolution of the mantle, *J. Geol.* 92, 497–523, 1992.
- [8] M.J. Bickle, Heat loss from the Earth: constraints on Archean tectonics from the relation between geothermal gradients and the rate of plate production, *Earth Planet. Sci. Lett.* 40, 301–315, 1978.
- [9] G.F. Davies, Thickness and thermal history of continental crust and root zones, *Earth Planet. Sci. Lett.* 44, 231–238, 1979.
- [10] G. Schubert, D. Stevenson and P. Cassen, Whole planet cooling and the radiogenic heat source contents of the Earth and Moon, *J. Geophys. Res.* 85, 2531–2538, 1980.
- [11] N.J. Vlaar, Precambrian geodynamical constraints, in: *The Deep Proterozoic Crust in the North Atlantic Provinces*, A.C. Tobi and J.L.R. Touret, eds., Reidel, 1985.

- [12] F.D. Stacey, *Physics of the Earth*, Wiley, New York, 1977.
- [13] H.N. Sharpe and W.R. Peltier, Parameterized mantle convection and the Earth's thermal history, *Geophys. Res. Lett.* 5, 737–740, 1978.
- [14] M.J. Jackson and H.N. Pollack, On the sensitivity of parameterized convection to the rate of decay of internal heat sources, *J. Geophys. Res.* 84, 10103–10108, 1984.
- [15] M.J. Jackson and H.N. Pollack, Mantle devolatilization and convection: implications for the thermal history of the earth, *Geophys. Res. Lett.* 14, 737–740, 1987.
- [16] P.J. McGovern and G. Schubert, Thermal evolution of the Earth: effects of volatile exchange between atmosphere and interior, *Earth Planet. Sci. Lett.* 96, 27–37, 1989.
- [17] J. Weertman and J.R. Weertman, High temperature creep of rock and mantle viscosity, *Annu. Rev. Earth Planet. Sci.* 3, 293–315, 1975.
- [18] D.R. Williams and V. Pan, Internally heated mantle convection and the thermal and degassing history of the Earth, *J. Geophys. Res.* 97, 8937–8950, 1992.
- [19] J.G. Sclater, J. Jaupart and D. Galson, The heat flow through oceanic and continental crust and the heat loss of the Earth, *Rev. Geophys. Space Phys.* 18, 269–311, 1980.
- [20] N.H. Sleep, Thermal history and degassing of the earth: some simple calculations, *J. Geol.* 87, 671–686, 1979.
- [21] F.D. Stacey, The cooling Earth: a reappraisal, *Phys. Earth Planet. Inter.* 22, 89–96, 1980.
- [22] U. Hansen and A. Ebel, Experiments with a numerical model related to mantle convection: boundary layer behaviour of small- and large-scale flows, *Phys. Earth Planet. Inter.* 36, 374–390, 1984.
- [23] V. Steinbach, *Numerische Experimente zur Konvektion in kompressiblen Medien*, Ph.D. Thesis, Univ. Cologne, 1991.
- [24] B.H. Hager, Subducted slabs and the geoid: constraints on mantle rheology and flow, *J. Geophys. Res.* 89, 6003–6016, 1984.
- [25] A. Chopelas and R. Boehler, Thermal expansion measurements at very high pressure, systematics and a case for a chemically homogeneous mantle, *Geophys. Res. Lett.* 16, 1347–1350, 1989.
- [26] M. Osaka and E. Ito, Thermal diffusivity of MgSiO<sub>3</sub> perovskite, *Geophys. Res. Lett.* 18, 239–242, 1991.
- [27] U.R. Christensen, Heat transport by variable viscosity convection and implications for the Earth's thermal evolution, *Phys. Earth Planet. Inter.* 35, 264–282, 1984.
- [28] U.R. Christensen, Thermal evolution models for the Earth, *J. Geophys. Res.* 90, 2995–3008, 1985.
- [29] N.J. Vlaar and A.P. van den Berg, Continental evolution and archaeo-sea-levels, in: *Glacial Isostasy, Sea-level and Mantle Rheology*, R. Sabadini, K. Lambeck and E. Boschi, eds., Kluwer, Dordrecht, 1991.
- [30] D.P. McKenzie, The generation and compaction of partially molten rock, *J. Petrol.* 25, 713–765, 1984.
- [31] E. Takahashi, Speculations on the Archean mantle: missing link between komatiite and depleted garnet peridotite, *J. Geophys. Res.* 95, 15941–15954, 1980.
- [32] D. McKenzie and M.J. Bickle, The volume and composition of melt generated by the extension of the lithosphere, *J. Petrol.* 29, 625–679, 1988.
- [33] D. Abbott, L. Burgess, J. Longhi and W.H.F. Smith, An empirical thermal history of the Earth's upper mantle, *J. Geophys. Res.*, submitted, 1993.
- [34] A.L. Jaques and D.H. Green, Anhydrous melting of peridotite at 0–15 kb pressure, *Contrib. Mineral. Petrol.* B73, 287–310, 1980.
- [35] R. Jeanloz, Thermodynamics of phase transitions, *Rev. Mineral.* 14, 389–429, 1985.
- [36] G.H. Miller, E.M. Stolper and T.J. Ahrens, The equation of state of a molten komatiite 2. Application to komatiite petrogenesis and the Hadean mantle, *J. Geophys. Res.* 96, 11849–11864, 1991.
- [37] M.J. O'Hara, M.J. Saunders and E.L.P. Mercy, Garnet-peridotite, primary ultrabasic magma and eclogite: interpretation of upper mantle processes in kimberlite, *Phys. Chem. Earth* 9, 571–604, 1975.
- [38] E.G. Nisbet, *The Young Earth: An Introduction to Archaean Geology*, Allen and Unwin, London, 1987.
- [39] D.J. Stevenson, Formation and early evolution of the Earth, in: *Mantle Convection*, W.R. Peltier, ed., pp. 818–873, Gordon and Breach, New York, 1989.
- [40] N.J. Vlaar, The driving mechanism of plate tectonics: a qualitative approach, in: *Progress in Geodynamics*, G.J. Borradaile et al., eds., North Holland, Amsterdam, 1975.
- [41] N.J. Vlaar and M.J.R. Wortel, Lithospheric aging, instability and subduction, *Tectonophysics* 32, 331–351, 1976.
- [42] E.R. Oxburgh and E.M. Parmentier, Compositional and density stratification in oceanic lithosphere—causes and consequences, *J. Geol. Soc. London* 133, 343–355, 1977.
- [43] P.F. Hoffman and G. Ranalli, Archaean oceanic plate tectonics, *Geophys. Res. Lett.* 15, 1077–1080, 1988.
- [44] R.J. O'Connell and B.H. Hager, in: *Physics of the Earth's Interior*, A.M. Dziewonski and E. Boschi, eds., pp. 270–317, Elsevier, New York, 1980.
- [45] P.E. van Keken, C.J. Spiers, A.P. van den Berg and E.J. Muzert, The effective viscosity of rocksalt: implementation of steady-state creep laws in numerical models of salt diapirism, *Tectonophysics* 225, 457–476, 1993.
- [46] P.E. van Keken, Numerical modelling of thermochemically driven fluid flow with non-Newtonian rheology applied to the Earth's lithosphere and mantle, Ph.D. Thesis, Univ. Utrecht, 1993.
- [47] U. Christensen and D.A. Yuen, The interaction of a subducting lithospheric slab with a chemical or phase boundary, *J. Geophys. Res.* 89, 4389–4402, 1984.
- [48] A.E. Ringwood, *Composition and petrology of the Earth's Mantle*, McGraw-Hill, New York, 1975.
- [49] T.J. Ahrens and G. Schubert, Gabbro–eclogite reaction rate and its geophysical significance, *Rev. Geophys. Space Phys.* 13, 383–400, 1975.

- [50] M. Ogawa, Numerical experiments on coupled magmatism–mantle convection system: implications for mantle evolution and Archean continental crust, *J. Geophys. Res.* 93, 15119–15134, 1988.
- [51] H. Fukuyama, The heat of fusion of basaltic magma, *Earth Planet. Sci. Lett.* 73, 407–414, 1985.
- [52] N.T. Arndt and E.G. Nisbet, eds., *Komatiites*, Allen and Unwin, London, 1982.
- [53] K.C. Condie, Archean geotherms and supracrustal assemblages, *Tectonophysics* 105, 29–41, 1984.
- [54] H. Austrheim, Eclogite formation and dynamics of crustal roots under continental collision zones, *Terra Nova* 3, 492–499, 1991.
- [55] P. Machetel and D.A. Yuen, Penetrative convective flows induced by internal heating and mantle compressibility, *J. Geophys. Res.* 94, 10609–10626, 1989.
- [56] V. Steinbach and D.A. Yuen, The effects of multiple phase transitions on Venusian mantle convection, *Geophys. Res. Lett.* 19, 2243–2246, 1992.
- [57] L.H. Kellogg, Interactions of plumes with a compositional boundary at 670 km, *Geophys. Res. Lett.* 18, 865–868, 1991.
- [58] U. Hansen, V. Steinbach and D.A. Yuen, The dynamics at internal boundaries in an Earth's mantle with depth-dependent material properties, *Terra Nova* 5, 101, 1993 (EUG VII Suppl.).
- [59] P.E. van Keken, D.A. Yuen and A.P. van den Berg, Pulsating diapiric flows: Consequences of vertical variations in mantle creep laws, *Earth Planet. Sci. Lett.* 112, 179–194, 1992.
- [60] U. Hansen and D.A. Yuen, High Rayleigh number regime of temperature-dependent viscosity convection and the Earth's early thermal history, *Geophys. Res. Lett.* 20, 2191–2194, 1993.
- [61] E.M. Klein and C.H. Langmuir, Global correlations of ocean ridge basalt chemistry with axial depth and crustal thickness, *J. Geophys. Res.* 92, 8089–8115, 1987.
- [62] V. Steinbach, D.A. Yuen and W. Zhao, Instabilities from phase transitions and the timescales of mantle thermal evolution, *Geophys. Res. Lett.* 20, 1119–1122, 1993.
- [63] M.J.R. Wortel, M.J.N. Remkes, R. Govers, S.A.P.L. Cloetingh and P.Th. Meijer, Dynamics of the lithosphere and the intraplate stress field, *Philos. Trans. R. Soc. London A* 337, 111–126, 1991.